COMPEL - The international journal for computation and mathematics in electrical and electronic engineering

Numerical studies of the melting process in the induction furnace with cold crucible

A. Umbrasko, E. Baake, B. Nacke, A. Jakovics,

Numerical studies of the melting process in the induction furnace with cold crucible

A. Umbrasko, E. Baake and B. Nacke
Institute for Electrothermal Processes, University of Hanover, Hanover, Germany, and
A. Jakovics
Laboratory for Mathematical Modelling of Environmental and Technological Processes, University of Latvia, Riga, Latvia

Abstract
Purpose – Aims to present recent activities in numerical modeling of cold crucible melting process.

Design/methodology/approach – 3D numerical analysis was used for electromagnetic problem and 3D large eddy simulation (LES) method was applied for fluid flow modeling.

Findings – The comparative modeling shows, that higher H/D ratio of the melt is more efficient when total power consumption is considered, but this advantage is held back by higher heat losses through the crucible walls. Also, calculations reveal that lower frequencies, which are energetically less effective, provide better mixing of the melt.

Originality/value – 3D electromagnetic model, which allows to take into account non-symmetrical distribution of Joule heat sources, together with transient LES fluid flow simulation gives the opportunity of accurate prediction of temperature distribution in the melt.

Keywords Melting, Simulation, Numerical analysis, Modelling, Furnaces

Paper type Research paper

Introduction
Melting of high-purity cast products is often carried out in induction furnace with cold crucible (IFCC), which offers various technological and economical advantages like melting, alloying and casting in one process step. Owing to its importance for modern industry it has become the subject for numerical modeling (Baake *et al.*, 2001; Bojarevics *et al.*, 2003; Fort *et al.*, 2005). The main distinguishing feature is that melt is kept in the water-cooled crucible and, therefore, high purity of material is assured by solid skull layer at the melt-crucible contact zone. Practical experiences show that the overheating temperature of the entire melt, which is determined by the electromagnetic, hydrodynamic and thermal process factors, is one of the key parameters of this technological process. The task of optimizing melt overheating faces the challenge of finding optimal combination of crucible height to diameter ratio, number of inductor turns and crucible sections, current strength and frequency. Changing of any mentioned factor influences the shape of melt meniscus and, as a result, flow pattern and energy balance. Therefore, solving of this problem should be

Part of this work was carried out with the IBM pSeries supercomputer of the HLRN and the authors thank all members from the HLRN for their support. Also this work has been supported by the European Social Fund.

COMPEL: The International Journal for Computation and Mathematics in Electrical and Electronic Engineering
Vol. 27 No. 2, 2008
pp. 359-368

0332-1649
DOI 10.1108/03321640810847643

based on determination of main tendencies for given direction of parameter change. This could be done performing numerical calculations for series of process configurations, with only one of parameters being varied.

Former experimental investigations show, that rotational flow structures driven by electromagnetic forces are often unstable. Resulting intensive flow oscillations are thought to be responsible for improved heat and mass transfer between different flow regions. Commonly used 2D numerical models based on the Reynolds-averaged Navier-Stokes (RANS) equations cannot describe this phenomenon and therefore usually predict temperature distribution which deviates from measurement results. Major reason of imprecision of 2D models is the 3D character of real flow oscillations. Logically, if we would like to avoid developing of empirical parameter set in order to adjust our 2D model for particular flow case, using of 3D modeling approach is obligatory. The large eddy simulation (LES) method, which is receiving growing attention at the present time and is actually being used for practical applications (Thomas *et al.*, 2001; Horvat *et al.*, 2001; Kohno and Tanahashi, 2002), was chosen for our numerical studies of cold crucible melting process. Our model experiments in crucible induction furnace have shown applicability of LES to the discussed flow category, not only providing good agreement in terms of calculated flow pattern, but also confirming experimentally determined characteristics of flow oscillations (Umbrashko *et al.*, 2006).

Electromagnetic model of cold crucible

Figure 1 shows the photo of our experimental IFCC with inductor, slit crucible and melt. It looks axis-symmetric, but it is not exactly so, because of the gaps in the crucible wall.

Figure 1.
Induction furnace with cold crucible

Since, the crucible is made of conducting material, the eddy currents are excited in the slits and they significantly influence electromagnetic field distribution. Therefore, 2D simulations of IFCC should take into account this phenomenon. There are several ways to do this: implement the effective magnetic permeability of the crucible material, or estimate the eddy currents in the walls. The use of mentioned approximations is complicated by the fact, that the amount of melt in the crucible and its shape changes the field as well. Hence, the qualitative estimations, which are suitable for one system, may produce incorrect results for another. Also the evaluation of power balance in the system may be misleading, because in reality significant amount of the electrical losses belongs to the slit crucible (about 50 percent). 2D model does not calculate these losses directly.

Initially we have used 2D approximation taking into account the ratio between the crucible section and gap width. This approach was tuned for our experimental installation and was used for the series of calculations with varied diameter of the crucible; it will be described later. Main advantage is the short solution time, which is significant for the iterative process of meniscus shape calculation.

However, the constant growth of the computational power allows us to perform the 3D calculations on the common workstation. The 3D simulation with sufficient mesh resolution can be completed within reasonable time period. We have used the commercial software ANSYS for this purpose.

Our experimental IFCC, which was modeled, is built of 14 segments and has the inner crucible diameter of 16 cm. The five-turn inductor height is about 20 cm and the operational power varies from 150 up to 200 kW. The 3D model contains a sector with half of crucible segment and half of the attached gap (Figure 2), which in our case corresponds to the 12.86° angle. The flux-parallel condition is applied on the side boundaries, but on the other boundary planes the vector-potential is set to zero. The current strength is applied to each inductor turn and its distribution inside the coil is calculated during the solution. The results of simulation contain induced currents in all conducting regions; therefore it is possible to calculate the total power losses in the whole system. The use of 3D electromagnetic model also brings another advantage, because it gives the non-symmetrical (real) Lorentz force and Joule heat distribution in the melt. Figure 3 shows how the intensity of Joule heat sources at the melt surface depends on the angular position for different heights.

The shape of the melt interface is calculated by establishing point-to-point balance of all involved forces. The equation is:

$$\rho g \Delta z - P_{\mathrm{EM}} - \gamma\left(\frac{1}{R_1} + \frac{1}{R_2}\right) = \Delta P \qquad (1)$$

where $P_{\mathrm{EM}} = B^2/2\mu$ is the electromagnetic pressure, γ is the surface tension coefficient and R_1, R_2 are the curvature radii. The surface profile is divided into the equal sections by the 40 nodes. Then the shape is adjusted in iterative way, until the ΔP becomes the same for each point. The electromagnetic calculations are performed on a 3D ANSYS model. The obtained magnetic field intensity data are used then by external code which makes shape adjustments.

Fluid flow modeling

The simulation of the fluid flow and thermal problem was done using LES numerical scheme. 3D calculations based on LES can be assumed as a compromise between the solving of RANS equations and direct numerical simulation (DNS). Main flow structure

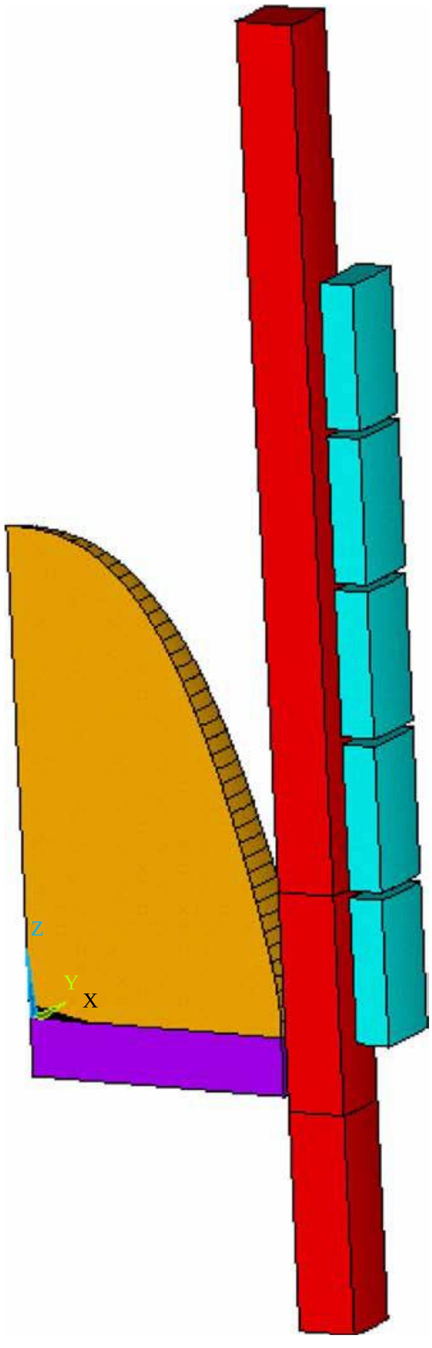

Figure 2.
3D ANSYS model of cold crucible installation

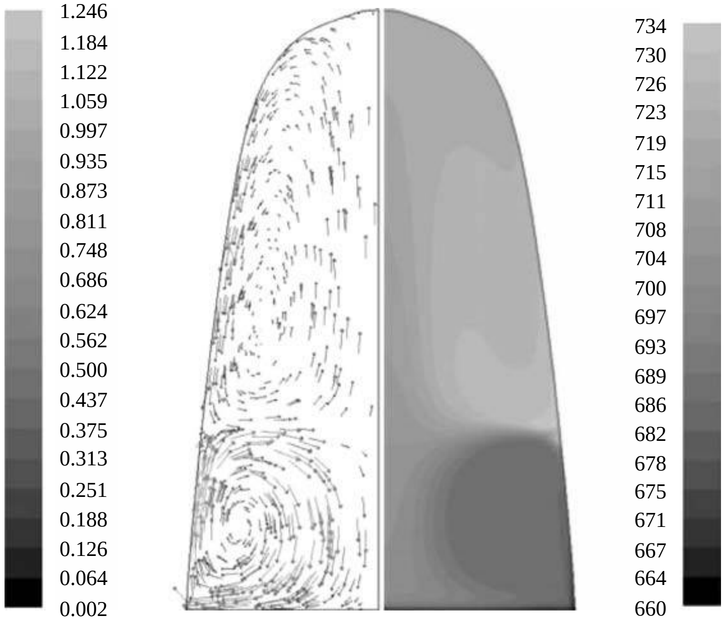

Figure 3.
Velocity (left, m/s) and temperature (right, ℃) distributions calculated with 2D k − ε model

is resolved directly like in the DNS approach, but small eddies, which size is comparable with grid size, are modeled additionally. Therefore, finer meshing and, as result, more computational resources are required in order to get an advantage over two-equation models, e.g. k-ε turbulence model, but still less than it is necessary for the application of the DNS. The sub-grid turbulent viscosity μ_{sub} was calculated with Smagorinsky-Lilly scheme used in FLUENT (Fluent 5 User's guide, 1999):

$$\mu_{\mathrm{sub}} = \rho L_s^2 |S_{ij}|, \quad L_s = \min\left(kd, C_s \sqrt[3]{V_{\mathrm{c}}}\right), \quad S_{ij} \equiv \frac{1}{2}\left(\frac{\partial u_i}{\partial x_j} + \frac{\partial u_j}{\partial x_i}\right) \tag{2}$$

where d is the distance from the closest wall, $k = 0.42$, $C_s = 0.1$ is the Smagorinsky constant and V_{c} is volume of the computational cell.

Owing to the transient mode of calculations, we have two significant simulation outcomes: time-averaged and time-dependent distributions of flow variables. First one is comparable with measured flow pattern, since it is difficult in practice to achieve any other snapshot of the flow. Numerical simulation with LES additionally gives us information about transient-flow development. This allows visualization and quantitative analysis of the convective transfer mechanisms.

Numerical model consisted of approximately 3×10^6 elements; this corresponds to the average cell size of ~ 1 mm. Boundary layer aligned at the surface had first element depth of ~ 0.2 mm. Transient calculations run with time-step in region of 5 ms. This combination of parameters ensured stable convergence within 5-10 iterations. Usually, it is necessary to simulate-flow development as long as several turn-around periods of the main vortexes. In this particular case about 15 s are sufficient for collecting enough data for time-averaging of the flow and temperature fields. It takes approximately 3-4 weeks on our four-workstation cluster for these calculations.

The former numerical investigations of cold crucible, based on 2D RANS methods, gave acceptable results for flow pattern (Figure 3 left), however they did not always agree with measured temperature distribution. Simulation predicted temperature gradients between dominating vortexes (Figure 3 right), which were not confirmed by the measurements (Figure 4 right). The time-average of the velocity field predicted with LES (Figure 4 left) was in agreement with both experiment and 2D results. At the same time, transient flow behavior shows intensive oscillations, which cause homogenization of temperature inside the whole melt.

Parameter studies for TiAl melt

The 3D numerical investigations of TiAl-melting process produced similar results in terms of time-averaged flow pattern (Figure 5 left). The melt mass was the same 6 kg,

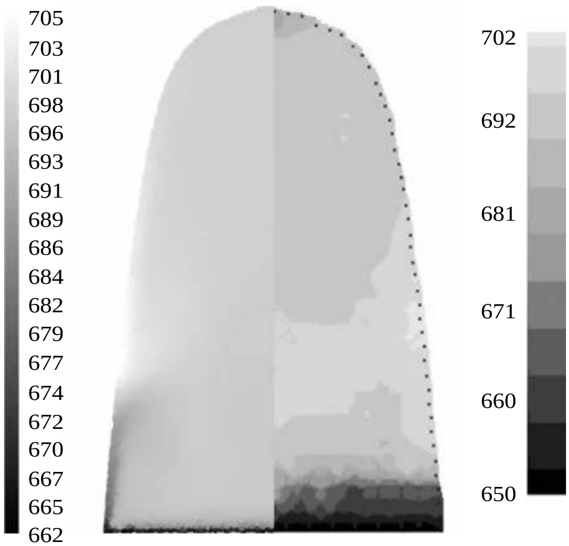

Figure 4.
Temperature distribution in aluminum melt in IFCC measured (right) and calculated with 3D LES turbulence model (left) (°C)

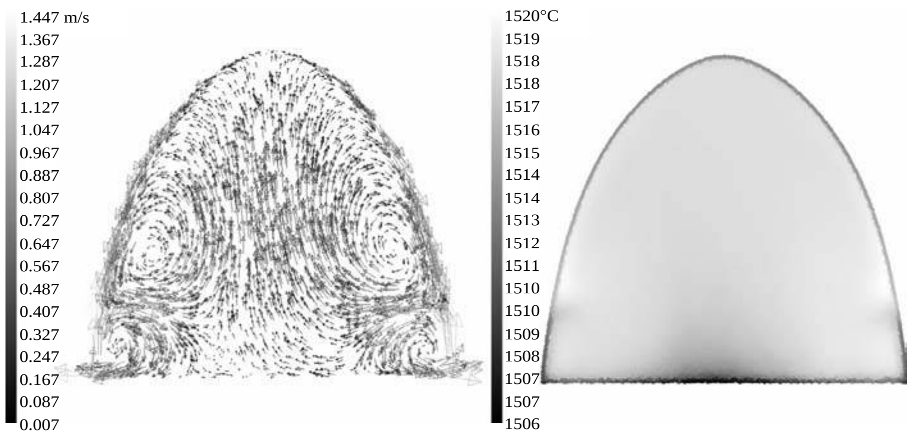

Figure 5.
Time-averaged velocity and temperature distribution in TiAl alloy calculated with LES turbulence model

but the meniscus height in this case is lower due to the increased density of the material. The flow velocities are slightly higher (maximal average velocity at $r = 0$ is about 55 cm/s), therefore the temperature distribution is more homogeneous, than in aluminum. Calculated temperature oscillations have similar amplitude (3-4 K) as these measured in aluminum (Figure 6). It should be taken into account here, that higher frequencies in measured oscillations are "filtered" by thermocouple, while the time step in the calculations was 0.01 s.

Owing to the noticeably lower H/D ratio of the melt shape, the low-velocity zone exists in the middle of the bottom region, which may lead to the thicker skull layer above the water-cooled base. Therefore, the modification of the crucible's geometry or load is considered as a possible way to improve the efficiency of the process.

There were performed calculations for the three different H/D ratios, but the power induced in the melt was kept the same. The Figure 5 shows the results for two ratios: 1.20 (left) and 1.67 (right) additionally to the 0.84 ratio shown on Figure 3. As it can be seen, the flow is more intensive near the central axis in case of smaller diameter crucible. This can prevent the formation of the thick layer of the solidified material at the bottom. But, at the same time, the melt has larger contact area with the crucible walls, which can lead to the changes in the electromagnetic forces and Joule heat sources distribution in the melt, as well as to increased heat flux to the water-cooled slits. But, the comparison of electrical efficiency of these systems show (Table I), that only about 18 percent of the full power are induced in the melt in case of H/D $= 0.84$, while for the larger ratio it is ~ 36 percent.

Also, the influence of the electromagnetic field frequency was studied. The Figure 6 shows the melt shape and the time-averaged flows for two cases: 5 and 20 kHz. The melt height decreases at higher frequencies (the induced Joule heat was kept almost constant, see Table II). The velocities are noticeably smaller in the 20 kHz case (almost twice on the axis), which may lead to the less intensive mixing. These particular

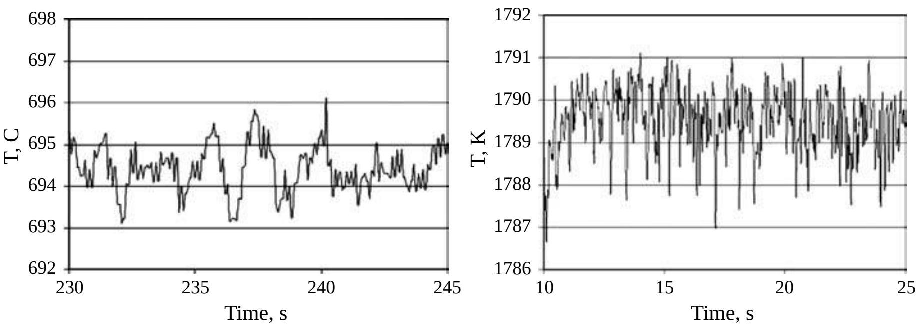

Figure 6. Temperature oscillations on the axis measured in aluminum (left) and calculated for TiAl alloy with LES turbulence model (right)

Ratio of the melt (H/D)	Inductor current (kA)	Total power (kW)	Power in the melt (kW)	Power in the melt (percent)
0.84	4.6	275.3	50	18.2
1.20	4.0	188.0	50	26.6
1.67	3.7	138.6	50	36.1

Table I. Parameter studies of height/diameter ratio influence on TiAl melting process in IFCC calculations show, that maximum temperature for 20 kHz is by 7 K (or 28 percent from temperatures range in the melt) higher then for 5 kHz. This can be considered advantageous, because increasing of the overheating temperature is useful for practical applications (Figures 7 and 8).

Following stage of investigations included usage of 3D Joule heat sources distribution in fluid flow calculations. This means that sources intensity varies periodically in azimuthal direction with noticeable maximums at the middle of the slits. This approach slightly influenced the temperature distribution (Figure 9). There can be

Table II.
Parameter studies of current frequency influence on TiAl melting process in IFCC

Frequency (kHz)	Ratio of the melt (H/D)	Inductor current (kA)	Total power (kW)	Power in the melt (kW)	Power in the melt (percent)
5	0.96	6.5	171	36	21
10	0.82	5.0	179	39	22
20	0.74	4.0	186	45	24

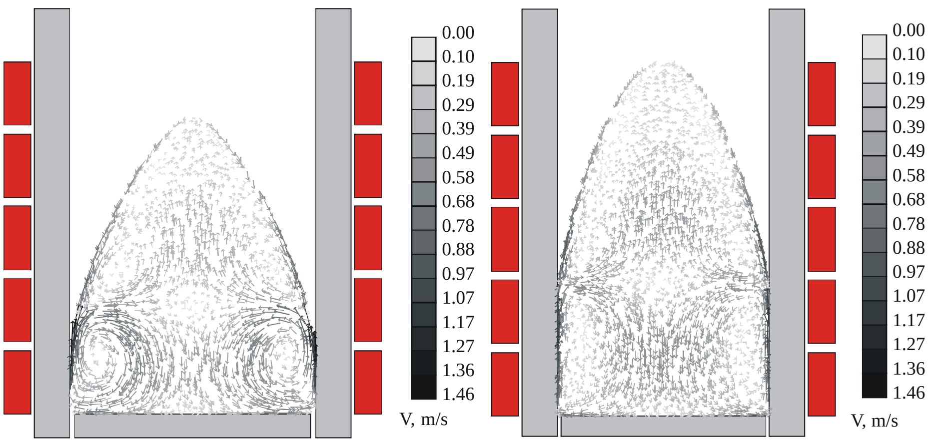

Figure 7.
Velocity vectors of TiAl melt in cold crucible with H/D ratios 1.20 (left) and 1.67 (right)

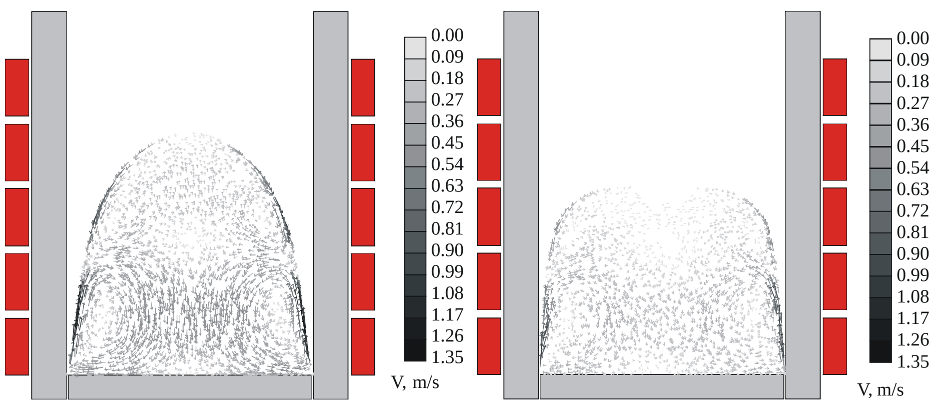

Figure 8.
Velocity vectors of TiAl melt in cold crucible with e-m field frequency 5 kHz (left, H/D = 0.99) and 20 kHz (right, H/D = 0.77)

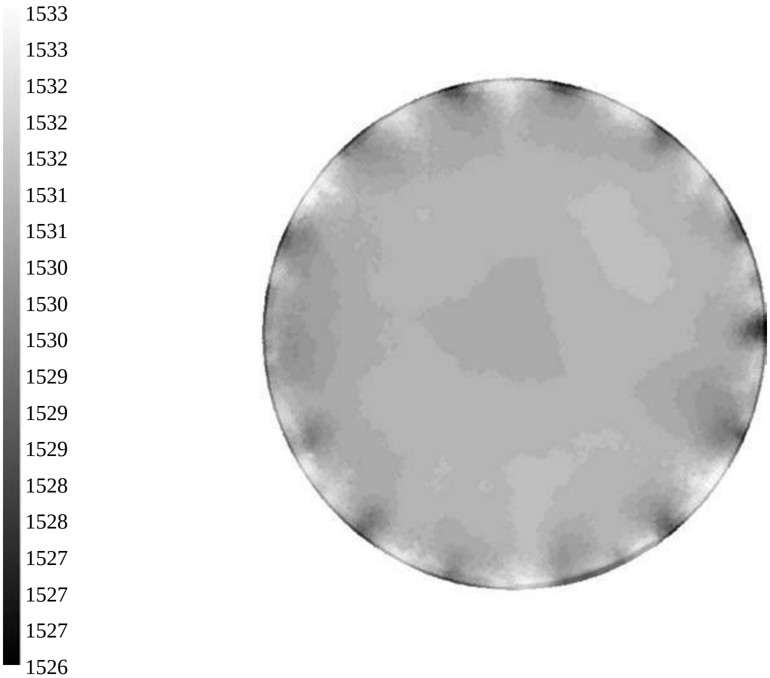

Note: 3D Joule heat sources and Lorentz forces were used

Figure 9.
Time-averaged temperature distribution (°C) in the horizontal cut calculated with LES model

seen periodic temperature variations in the surface zone if we look from above to the cross-sections, which are parallel to the crucible bottom. During the aluminum melting experiment this phenomenon can be observed as azimuthal-wave-like surface deformations of the meniscus.

Conclusions

The results of the LES modeling of aluminum-melting process are in good agreement with the results of experimental investigations.

The comparative modeling results show, that parameters configurations which provide higher H/D ratio of the melt are more efficient when total power consumption is considered, but this advantage is held back by higher heat losses through the crucible walls. Also, calculations reveal that lower frequencies, which are energetically less effective, provide better mixing of the melt. Considering, that change of any parameter (frequency, power, crucible radius) influences the melt shape and, therefore, the electromagnetic coupling and temperature distribution, further investigations are required to obtain the optimal IFCC configuration.

References

Baake, E., Nacke, B., Bernier, F., Vogt, M., Mühlbauer, A. and Blum, M. (2001), “Experimental and numerical investigations of the temperature field and melt flow in the induction furnace with cold crucible", *Proc. of the Int. Seminar on Heating by Internal Sources. Padua (Italy), September 12-14*, pp. 21-8.

Bojarevics, V., Djambazov, G., Harding, R.A., Pericleous, K. and Wickins, M. (2003), "Investigation of the cold crucible melting process: experimental and numerical study", *Magnetohydrodynamics*, No. 4, pp. 395-402.

Fluent 5 User's guide (1999), *10.7.2 Subgrid-Scale Models*, Fluent Inc., Lebanon, NH.

Fort, J., Garnich, M. and Klymyshyn, N. (2005), "Electromagnetic and thermal-flow modeling of a cold-wall crucible induction melter", *Metallurgical and Material Transactions B*, Vol. 36B, pp. 141-52.

Horvat, A., Kljenaka, I. and Marnb, J. (2001), "Two-dimensional large-eddy simulation of turbulent natural convection due to internal heat generation", *International Journal of Heat and Mass Transfer*, Vol. 44 No. 21, pp. 3985-95.

Kohno, H. and Tanahashi, T. (2002), "Finite element simulation of single crystal growth process using GSMAC method", *Journal of Computational and Applied Mathematics*, Vol. 149 No. 1, pp. 359-71.

Thomas, B.G., Yuan, Q., Sivaramakrishnan, S., Shi, T., Vanka, S.P. and Assar, M.B. (2001), "Comparison of four methods to evaluate fluid velocities in a continuous slab casting mold", *Iron Steel Inst. Jpn. Int.*, Vol. 41, pp. 1266-76.

Umbrashko, A., Baake, E., Nacke, B. and Jakovics, A. (2006), "Modeling of the turbulent flow in induction furnaces", *Metallurgical and Material Transactions B*, Vol. 37B, pp. 831-8.

Corresponding author
A. Umbrasko can be contacted at: umbrasko@ewh.uni-hannover.de

This article has been cited by:

1. Yaohua Yang, Ruirun Chen, Qi Wang, Jingjie Guo, Yanqing Su, Hongsheng Ding, Hengzhi Fu. 2018. Dominant dimensionless parameters controlling solute transfer during electromagnetic cold crucible melting and directional solidifying TiAl alloys. *International Communications in Heat and Mass Transfer* **90**, 56-66. [Crossref]
2. Sławomir Golak, Roman Przylucki, Jacek Smolka, Piotr Bulinski, Piotr Cieplinski. 2017. Influence of a cold crucible geometry parameters on electrical efficiency. *International Journal of Applied Electromagnetics and Mechanics* **32**, 1-8. [Crossref]
3. Piotr Buli?ski, Jacek Smolka, S?awomir Golak, Roman Przy?ucki, Micha? Palacz, Grzegorz Siwiec, Jakub Lipart, Ryszard Bia?ecki, Leszek Blacha. 2017. Numerical and experimental investigation of heat transfer process in electromagnetically driven flow within a vacuum induction furnace. *Applied Thermal Engineering* . [Crossref]
4. Shuhei Matsuzawa, Gaku Yoshikawa, Katsuhiro Hirata, Fumikazu Miyasaka, Yasuhiro Nakai, Masanori Tsuda, Yu Komemushi. 2015. Coupled 3-D Analysis Employing FEM and Particle Method—Experimental Verification of Cold Crucible Induction Melting. *IEEE Transactions on Magnetics* **51**:3, 1-4. [Crossref]
5. A. Smalcerz, B. Oleksiak, G. Siwiec. 2015. The Influence A Crucible Arrangement On The Electrical Efficiency Of The Cold Crucible Induction Furnace. *Archives of Metallurgy and Materials* **60**:3. . [Crossref]
6. Jieren Yang, Ruirun Chen, Hongsheng Ding, Jingjie Guo, Yanqing Su, Hengzhi Fu. 2013. Flow field and its effect on microstructure in cold crucible directional solidification of Nb containing TiAl alloy. *Journal of Materials Processing Technology* **213**:8, 1355-1363. [Crossref]
7. Jieren Yang, Ruirun Chen, Hongsheng Ding, Yanqing Su, Guo Jingjie, Feng Huang, Hengzhi Fu. 2013. Uniformity analysis of magnetic field in an electromagnetic cold crucible used for directional solidification. *COMPEL - The international journal for computation and mathematics in electrical and electronic engineering* **32**:3, 997-1008. [Abstract] [Full Text] [PDF]
8. Shuhei Matsuzawa, Katsuhiro Hirata, Takahiro Yoshimura, Gaku Yoshikawa, Fumikazu Miyasaka. 2013. Numerical Analysis of Cold Crucible Induction Melting Employing FEM and MPS Method. *IEEE Transactions on Magnetics* **49**:5, 1921-1924. [Crossref]
9. Jie-ren YANG, Rui-run CHEN, Hong-sheng DING, Yan-qing SU, Feng HUANG, Jing-jie GUO, Heng-zhi FU. 2012. Numerical calculation of flow field inside TiAl melt during rectangular cold crucible directional solidification. *Transactions of Nonferrous Metals Society of China* **22**:1, 157-163. [Crossref]